Vibration characteristics of a cylinder with asymmetries

Heye Xiao (1,2), Jie Pan (1) and Meiping Sheng (2)

(1) School of Mechanical Engineering, University of Western Australia, Crawley WA 6009, Australia

(2) College of Marine Engineering, Northwestern Polytechnical University, Xi'an Shaan 710072, China

ABSTRACT

Many structures have apparent symmetries, implying symmetrical mode shapes of vibration. Practically many of those structures show asymmetric mode shapes. Slight variations in structure geometry, boundary conditions and material properties are often the cause of such asymmetric vibration properties. In this paper, the finite element method is applied to analyze the vibration characteristics of a cylinder with a slightly varying diameter. The results indicate that some mode shapes of the cylinder vibration are very sensitive to the small diameter variation. The numerical results of the cylinder vibration are verified experimentally.

INTRODUCTION

Symmetric structures are commonly assumed in engineering modelling. Practically structural irregularities, resulting from manufacturing tolerances and material nonuniformities, may change the property of the structural symmetry, and even make them asymmetric. For example, the cross sections of any pipe may not be perfect circles as there are always slight fluctuations in the diameters or material properties of the cross sections. As a result, the seemingly symmetrical pipe is actually asymmetric. This phenomenon is often ignored and the cross section shapes are considered uniform along length in traditional vibration modelling of pipes. However, the phenomenon may have a significant impact on the structural vibration and corresponding sound radiation behavior. Therefore it is necessary to study the effect of the slight distortion in the cross sections on the vibration characteristics of a cylindrical shell.

Much effort has been devoted to study the influence of various types of imperfections or geometric asymmetries on the vibration characteristics of the otherwise symmetric structures. Laura et al. [1] used Rayleigh–Ritz and finite element methods to analyze the effect of circumferential variations in wall thickness on the eigenfrequencies and axisymmetric modes of a nonuniform ring. Hwang et al. [2] employed the Novozhilov's thin-shell theory and Rayleigh–Ritz analysis to study the free vibration of a thin ring with variations in the ring's in-plane cross sectional profile. Khurasia and Rewtant [3] used finite-element method to examine the free vibrations of a thin circular plate with an eccentric hole. Hasheminejad et al [4] employed the translational addition theorem to develop an exact 3D elasticity solution for free vibrations of a simply supported elastic circular cylinder (shear diaphragm) of finite length with an eccentrically located inner circular cavity.

In contrast with the nonuniform rings, relatively few researchers have investigated the effects of slight variation in the cross section diameter on the vibrational behavior of cylindrical shells. In this paper, the finite element method (FEM) is employed to develop an asymmetric model of a free-free cylinder with a slight fluctuation in diameter to compare its modal characteristics with that of a similar cylinder with a uniform diameter. The geometric parameters of the asymmetric cylinder are based on those measured of a real pipe used for the experimental verification.

Modal tests of the pipe are carried out to verify the accuracy of finite element model. Through comparisons between the experimental and FEM results, useful conclusions are drawn.

NUMERICAL MODEL

Modelling of asymmetric cylinder

A practical pipe often has slight variation in its diameter, meaning its cross sections are not circular rings of constant thickness. The largest diameter of cross sections at the two ends of the pipe may be also twisted with an angular displacement. Although these variations are too small to be inspected visually, they do exist. An example is shown in Figure 1, which is plotted based on the measured data of a steel pipe (see Appendix C). The length, average diameter and wall thickness of the pipe are respectively 1.2 m, 0.0161m and 7mm.

In Figure 1, the fluctuations of the internal and external radius of the pipe cross section around averaged radius for each end are displayed. It can be seen that radii of the cross sections vary: the maximum relative variation is 0.35mm. There are also about 10 degree rotational displacements between the cross sections. Because the cylinder is a continuous system, it is assumed that its cross section continuously rotates along the length of the cylinder. The geometric model of the cylinder is established by plotting the cross section formed by the experiment data at the top end and linearly rotating the cross section along its length until a 10 degree angle is achieved at the bottom end. This model and free-free boundary condition are then imported into ANSYS [5-6] and meshed by the solid 187 element, for finite element analysis. The finite element model is demonstrated as Figure 2. To compare with the dynamic characteristics of a uniform cylinder, a model with a perfect circle cross section in a perfect model twithout rotation is drawn and imported into ANSYS. In the perfect model without rotation, the max element size is 0.01m and total number of elements is 40790.The umber of element change to 40422 in the rotational and varying cross section model of

same element size. The elastic modulus, Poisson's ratio and density in both models are 2.1×10^{11}N/m^2 , 0.33 and 7.8×10^{3}kg/m^3 respectively.

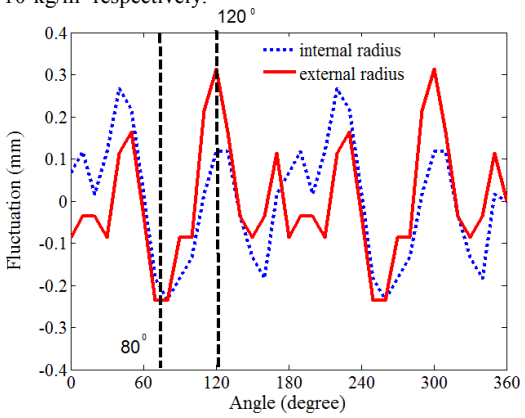

(a) top end of the pipe

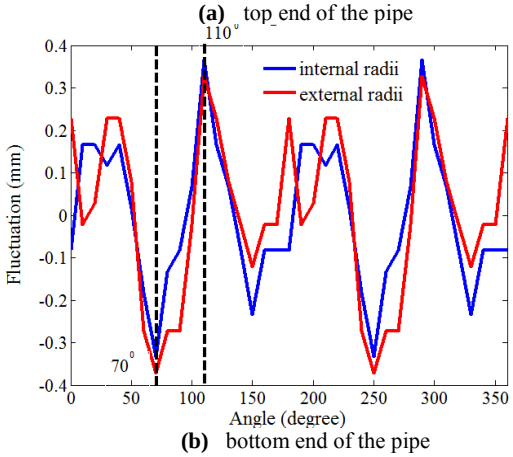

(b) bottom end of the pipe

Figure 1: Radius fluctuations around the average radius

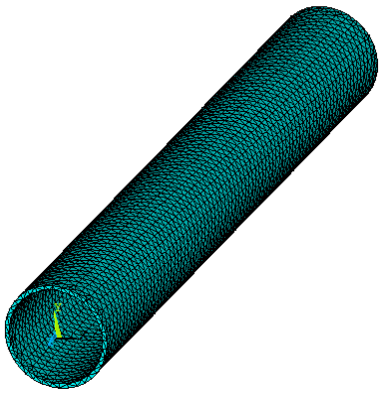

Figure 2: Finite Element model of the cylinder

Free vibration results

The vibration characteristics of the undamped cylinders are described by the natural frequencies and mode shapes. The first 10 natural frequencies of the two cylinders are calculated and compared in Table 1. Accordingly, the mode shapes of cylinders at those frequencies are extended to a plan style and plotted in Figures 3-6 and Figures A.2-A.7.

The out-of-plane modes of the cylinder are also summarised in Table 1, where n represents the circumferential number and m axial node number. Among the modes obtained, circumferential number n=1, 2, 3 and axial node number m=0, 1, 2, 3 were observed. The definition of n and m are given in reference [7].

Table 1 Natural frequencies of the uniform and asymmetric cylinders

Order	Natural frequency (Hz)		Node numbers (n,m)	figure number
	uniform cylinder	asymmetric cylinder		
1	659.7	657.32	(1,2)	Figure A1
2	659.7	662.31	(1,2)	Figure A2
3	724.07	716.66	(2,0)	Figure 3
4	724.18	723.58	(2,0)	Figure 4
5	727.93	720.76	(2,1)	Figure 5
6	728.06	727.39	(2,1)	Figure 6
7	779.6	775.3	(2,2)	Figure A3
8	779.69	780.34	(2,2)	Figure A4
9	985.28	982.28	(2,3)	Figure A5
10	985.35	985.37	(2,3)	Figure A6

We have found that the modes of the asymmetric and uniform cylinders can be directly compared. They are grouped in Table 1 in terms of the mode order and its node numbers.

For a given pair of node numbers (n, m), there are always two orthogonal modes. The natural frequencies and mode shapes of the asymmetric and uniform cylinder in the same group are compared below:

(a.1) For the asymmetric and uniform cylinder modes with the same order and node numbers of n, m=0 or n, m=1, the natural frequency of the asymmetric cylinder mode is always lower than that of the uniform cylinder mode.

(a.2) For the asymmetric and uniform cylinder modes with the same order and node numbers of (n, m= 2) or (n, m=3), the difference between natural frequencies of the asymmetric cylinder modes with the same node numbers is greater than that of the counterpart uniform cylinder. For this case, the lower natural frequency in the mode pair of the asymmetric cylinder becomes lower than that of the uniform cylinder mode, and the higher natural frequency becomes higher.

(a.3) For the modes of the uniform cylinder, either their axial node lines or anti-node lines start from zero degree of the coordinates. However for the modes of the asymmetric cylinder, their nodal lines or anti-nodal line have an angle off-set. In addition, the nodal lines or anti-nodal lines of some asymmetric cylinder modes even roll up or down by an angle. Taking the mode shapes in Figure A2 as an example, the first node line (red line) of the uniform cylinder starts at 0 degrees, while that of the asymmetric cylinder starts at 30 degrees. In Figure 4, the first node line of the asymmetric cylinder mode at L =0 is located at 30 degrees. Then the node line rolls down as the length increases: it is at 12 degrees at L=1.2m.

To show the relative change of the mode shapes between the asymmetric and uniform modes of the same order, the angu-

lar difference between the starting angle (measured at L = 0) of the first nodal line (red lines in Figures 3 to 6 and Figures A1 to A6) of the asymmetric cylinder and that of the uniform cylinder is defined as the shift angle. The relative angle between the starting and the ending of the first nodal line is defined as the rolling angle. All shift and rolling angles of the 10 modes are listed in Table 2.

(a.4) In Figure 1, it can be seen that the largest radius of the top end of the asymmetric cylinder occurs at 120 degrees. In reference [8], the anti-node lines or node lines of the mode shapes of a cylinder with variable circumferential profile always appears at the highest or lowest radius. The calculated node or anti-node lines of the asymmetric cylinder agree approximately with the observation made in [8]. For example, the first nodal line of the (1,2) asymmetric cylinder modes in Figure A1 is located at 30 degrees, and its first anti-node line is indeed located at 120 degrees.

Table 2. Shift and rolling angle of mode shapes of cylinders

Mode Order	Starting of the first node line		Shift Angle (degree)
	uniform cylinder	asymmetric cylinder	
	(degree)	(degree)	
1	90	120	30
2	0	30	30
3	45	75	30
4	0	30	30
5	45	75	30
6	0	30	30
7	45	70	25
8	0	24	24
9	45	35	-10
10	0	-10(80)	-10

Mode Order	asymmetric cylinder		Rolling Angle (degree)
	Starting of the first node line	Ending of the first node line	
	(degree)	(degree)	
1	120	120	0
2	30	30	0
3	75	69	6
4	30	12	18
5	75	63	12
6	30	27	3
7	70	70	0
8	24	24	0
9	35	35	0
10	-10(80)	-10(80)	0

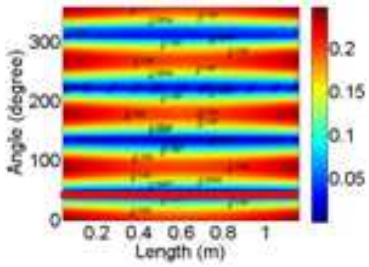

(a) uniform cylinder

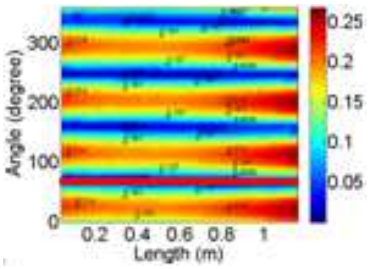

(b) asymmetric cylinder

Figure 3: Mode shapes of cylinders at the 3rd natural frequency

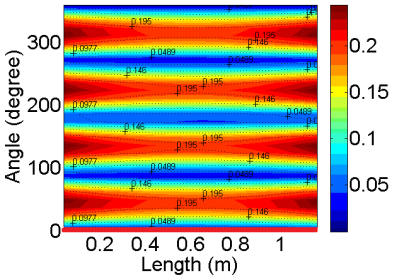

(a) uniform cylinder

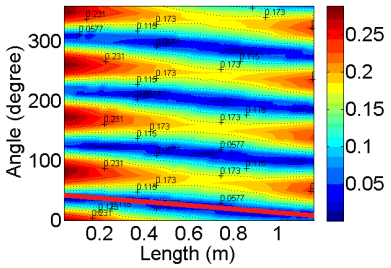

(b) asymmetric cylinder

Figure 4: Mode shapes of cylinders at the 4th natural frequency

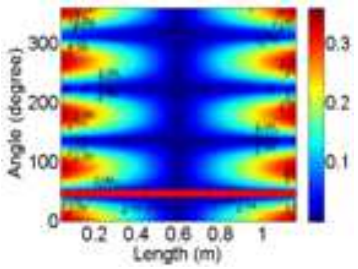

(a) uniform cylinder

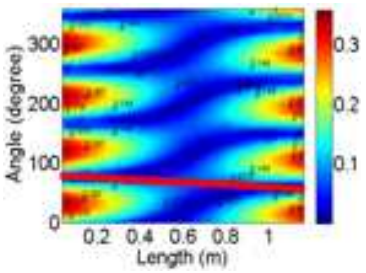

(b) asymmetric cylinder

Figure 5: Mode shapes of cylinders at the 5th natural frequency

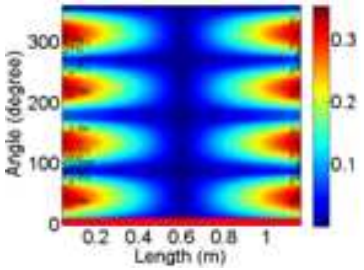

(a) uniform cylinder

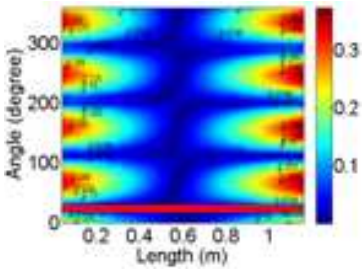

(b) asymmetric cylinder

Figure 6: Mode shapes of cylinders at the 6th natural frequency

(a.5) The alignment of the node and anti-node lines of the asymmetric cylinder in this paper, however, is more complicated than that in [8]. This is not only due to the relative angular shift of the profiles between the top and bottom cross sections, but also to the non-orthogonal angle between the directions for the maximum and minimum diameters of the cross sections.

As a result, although the angular alignments of the first two modes are very close to 120 degrees (30 degrees) at both ends of the cylinder, such alignment is not exact because of the angular shift between maximum diameters at two ends. As the relative value of the angular shift between node and anti-node of the lower order modes is small, the exact alignment is difficult to determine. This also applies to higher order modes (for modes 7-10) of the asymmetrical cylinder. However, the observed angular alignment becomes quite different to that indicated in [8]. For this case, angular alignments of mode shapes are close to 70 degrees (25 degrees) and 80 degrees (35 degrees) at both ends of the cylinder. Based on the above results, it is concluded that anti-node lines and node lines in the alignment of the cylinder at those modes probably align closely with the angular positions of maximum and minimum radius of the two ends. Such alignment must be due to the effect of the relative shift of the angles for the maximum diameters between the top and bottom sections and irregular profiles in the diameters. Nevertheless, future work is required to focus on the reasons causing the angular alignment of the modes.

For the modes with axial node number below 2, their angular alignments at the two ends of the cylinder are significantly different. This phenomenon was not covered in [8]. For the 3rd mode, it starts at 75 degrees at the top end and ends at 69 degree at the bottom end. So the alignments at the two ends differ by 6 degrees. For the 4th mode, it starts at 30 degrees and stops at 12 degrees. Anti-nodes at two ends of above modes' alignment are in-phase. For the 5th mode, the angular alignment changes from 75 degrees at the top end to 63 degrees at the bottom end. For the 6th mode, it changes from 30 degrees to 27 degrees. Along the alignment, the anti-nodes of the two modes at the two ends of cylinder are out of phase.

Qualitatively the circumferential stiffness distribution of the cylinder is no longer the same along the length as the cylinder's diameter profile varies with length. Therefore the vibration velocities must adjust their distribution at each ferquency to satisfy the requirement of the minimum energy principle. Finite element analysis is based on Hamiton's minimum energy principle and demonstrated that the unique way for the cylinder to obey this principle is to adjust the node lines or anti-node lines of mode shapes so that they roll from the top end to the bottom end with a specific starting angle and rolling angle.

EXPERIMENT RESULTS

The pipe, whose measured geometric details are shown in Appendix C, is selected for experimental analysis. It is suspended by two steel cables through 4 holes in the top end. The outside surface of the pipe is divided into 12×20 subareas of equal size. The circumference of each cross section is equally divided by 12 points, and the total length of pipe is equally covered by 21 points. Thus, all together, 252 measurement points are selected on the pipe surface. The numbering of the position begins from the welding line and increases clockwise from the top end to the bottom end of the pipe (see Figure 7).

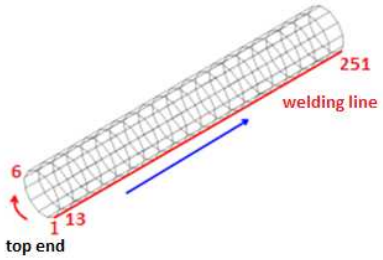

Figure 7: Distribution of test positions

In the experiment, the natural frequencies and mode shapes are obtained using the impulse method, which involves the measurement of the impact force using an impact hammer at bottom of the cylinder near test point number 220 and the acceleration using accelerometers at all the test positions. As two accelerometers were used, the tests were repeated so that the different positions could be measured. Charge amplifiers, data acquisition card and signal processing software in a computer are used to extract the natural frequencies and mode shapes of the cylinder. The set up of the experiment is shown in Figure 8.

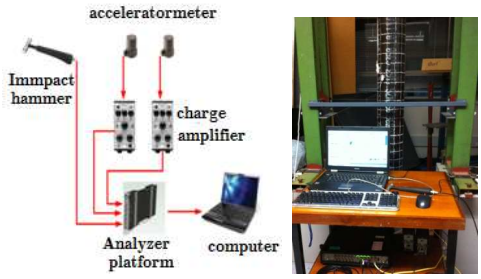

Figure 8. Experimental setup

At each measuring point, the acceleration and impulse force were measured simultaneously. They yield the Frequency Response Function (FRF) which is used to identify resonance frequencies and mode shapes.

The sampling frequency for the modal testing is 6400Hz. Attention was focused on the frequency range below 1000Hz, where the first 6 modes are located. The spatial averaged FRF functions of the cylinder are presented in Figure 9. Together with the mass of the cylinder, the averaged FRF represents the spatial averaged vibration energy with respect to one unit force of excitation on the pipe.

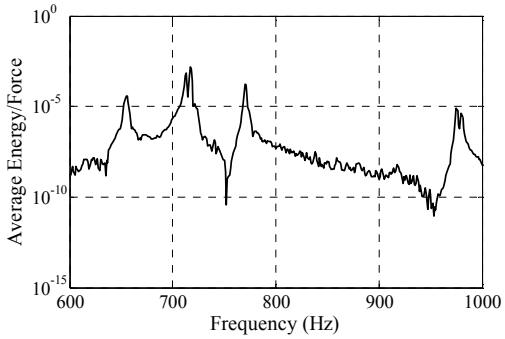

Figure 9: Average energy of the cylinder with respect to the driving force

From the spatial averaged energy response, the resonance peaks can be readily identified. Comparing these results with the simulation results, the experimental natural frequencies are identified and listed in Table 3. Corresponding to each frequency, the amplitude and phase information were extracted to plot the modal shapes. To obtain a better understanding of the test results, the corresponding mode shapes of the cylinder obtained experimentally are also displayed in plan view, shown as Figures 10-11 and Figures B1-B4. Node number of each mode is also listed in Table 3 for an easy comparison between the simulated and tested mode shapes.

Table 3: Measured natural frequencies of cylinder

Order Number	Frequency (Hz)	Node Number (n,m)	Figure Number
1	656	(1,2)	Figure B1
2	-	-	-
3	-	-	-
4	712	(2,0)	Figure 10
5	717	(2,1)	Figure 11
6	-	-	-
7	770	(2,2)	Figure B2
8	-	-	-
9	975	(2,3)	Figure B3
10	980	(2,3)	Figure B4

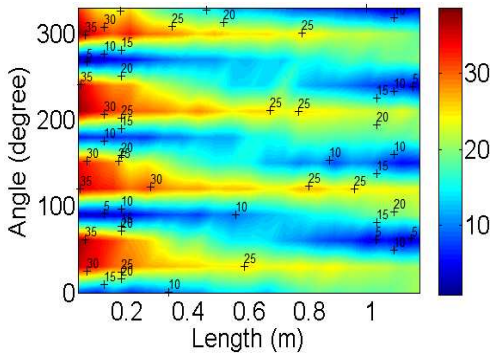

Figure 10: Measured mode shape at the 4th natural frequency

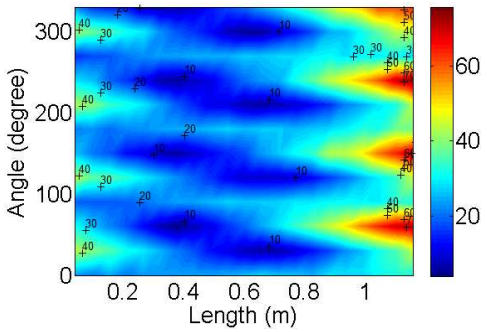

Figure 11: Measured mode shape at the 5th natural frequency

We have the following observations from the experimental results:

(b.1) It has been shown in FEM calculation that the two modes with the same nodal numbers have their natural frequencies closely located. As a result, the measurement of the mode shapes at those natural frequencies is dependent on the location of driving force. If the driving force is located near the nodal point of the mode, this mode may not be excited and therefore its mode shape and even its natural frequency may not be observed clearly. This might be the reason why the 2nd , 3rd , 6th and 8th modes are not identified. Furthermore, the drive point may be between the antinode and node of two orthogonal modes whose frequencies are close to each other. In this case, the responses contributed from two modes are almost equal even at one of their natural frequencies. It will then be difficult to distinguish the individual mode contribution. This might be the case for the measured mode shape at the 4th natural frequency. This is perhaps the other reason why four modes disappeared in the experiment.

(b.2) The natural frequencies with the same node number depart from each other. The mode shapes rotate from one end to other end, when m=0 or 1 in support of the simulation.

(b.3) Differences between the natural frequencies of the simulation and test results with same mode shape is very small and increase slightly with rise in frequency.

(b.4) Because there is no experimental data for the uniform cylinder, tested mode shapes and mode shapes of the uniform cylinder in simulation are selected to reveal experimentally the alignment of the node/anti-node lines based on the cross section profile and relative angular shift of the node/anti-node lines between the top and bottom ends. All results are listed and compared to simulation results in Table 4. Although there is obvious difference between results in simulation and experiment, the alignment of the node/anti-node lines and relative angular shift between the two sections at the ends are confirmed.

Every cross section of cylinder is divided into 12 parts in experiment. The smallest distinguishable unit of change in angle of mode shape is thus 30 degrees. Hence, if the shift and rolling angle of mode shape are smaller than 30 degree, some of them may not be recognized in the test. This is the main reason why translational shift of mode shape in the experiment results and those in the calculation have great differences.

Table 4: Shift and rolling angles in simulation and measurement results

Order	Shift Angle (degree)		Rolling Angle(degree)	
	experiment	simulation	experiment	simulation
1	30	30	0	0
4	0	30	30	18
5	0	30	30	12
7	0	25	0	0
9	-15	-10	0	0
10	-30	-10	0	0

(b.5) The simulation and test results demonstrates that even a 0.4% fluctuation in diameters of cylinder can generate the deterministic change in vibration characteristics, like mode shape rolling from the top end to the bottom end by 30 degree. To understand the modal details of the structure, such as the asymmetric cylinder considered here, the effect of the cross section profile and relative angular shift between the cross sections must be taken into account.

CONCLUSIONS

This paper presents a model which can be used to analyse effects of slight fluctuations in diameter of cylinder on its dynamic characteristics. The model used the finite element method based on the geometric parameters of a real pipe. All the results were compared with those of uniform cylinder model in which difference of diameter are neglected. Both variations in diameters and rotation of the profiles along the length of the pipe were included. It is concluded that natural frequencies with same node number are divided into two different frequencies after considering slight changes in geometry of cylinder. The mode shapes shift an angle for each mode. Mode shapes rolling from one end to the other occur, when m numbers of them are equal to 0 or 1. Finally, modal testing of the pipe whose parameters used in the simulation was carried out and the results in the experiment and simulation were close. It was demonstrated that model built in this paper is accurate and slight changes in diameter of a cylinder should be considered in establishing the dynamic model of real cylinder.

ACKNOWLEDGEMENTS

We thank Dr. Andrew Guzzomi for proof reading the manuscript and useful suggestions. Financial support from Chinese Ministry of Education, WA Acoustical Society and Centre for Acoustics, Dynamics and Vibration are gratefully acknowledged.

APPENDIX A

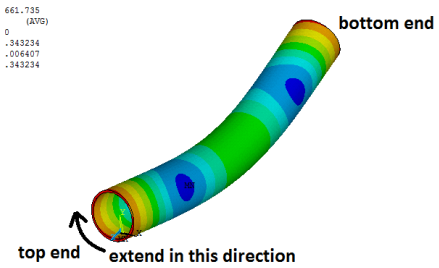

Figure A1: 3D view of the 1st natural frequency

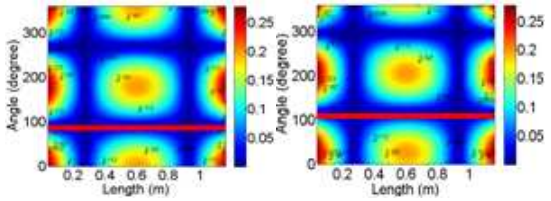

(a) uniform cylinder (b) asymmetric cylinder

Figure A2: Mode shapes of cylinders at the 1st natural frequency

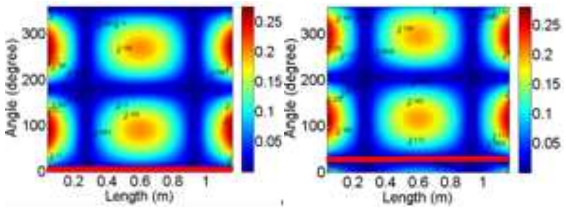

(a) uniform cylinder (b) asymmetric cylinder

Figure A3: Mode shapes of cylinders at the 2nd natural frequency

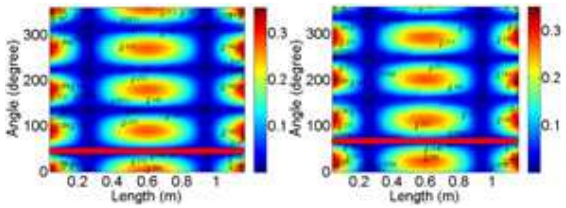

(a) uniform cylinder (b) asymmetric cylinder

Figure A4: Mode shapes of cylinders at the 7th natural frequency

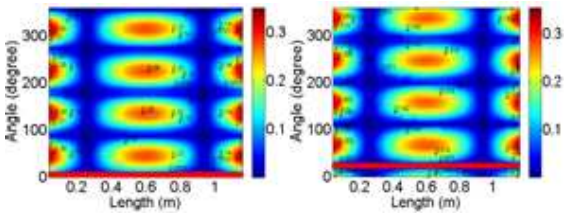

(a) uniform cylinder (b) asymmetric cylinder

Figure A5: Mode shapes of cylinders at the 8th natural frequency

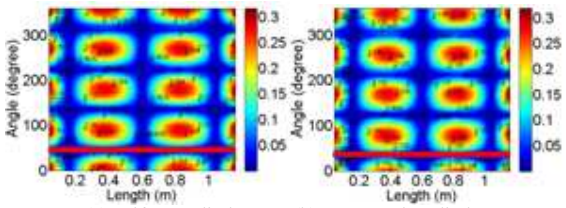

(a) uniform cylinder (b) asymmetric cylinder

Figure A6: Mode shapes of cylinders at the 9th natural frequency

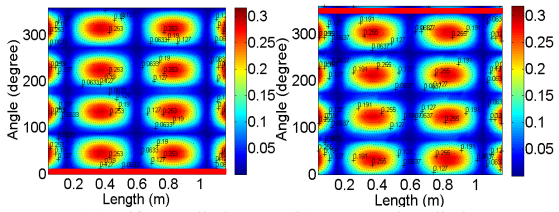

(a) uniform cylinder (b) asymmetric cylinder

Figure A7: Mode shapes of cylinders at the 10th natural frequency

APPENDIX B

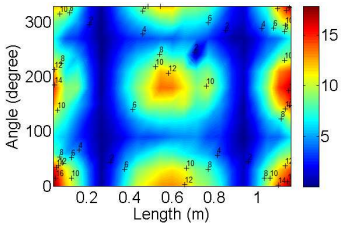

Figure B1: Measured mode shape at the 1st natural frequency

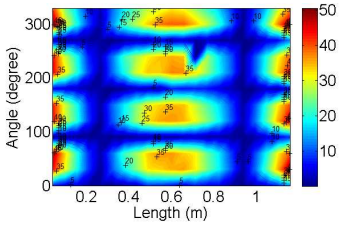

Figure B2: Measured mode shape at the 7th natural frequency

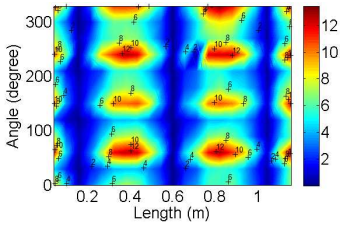

Figure B3: Measured mode shape at the 9th natural frequency

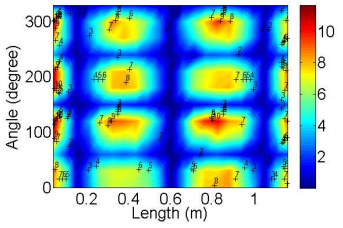

Figure B4: Measured mode shape at the 10th natural frequency

APPENDIX C

The size of the pipe for the test is 1.2m in length, 0.17 m in outside diameter and 0.007m in wall thickness. The cylinder has a welding line as shown in Figure C.1. Vernier callipers are used to measure the inside and outside diameters of the top end and bottom cross sections per 10 degree starting from the weld. Details of this measurement are plotted in Figure C.2 and all results are listed in Table C.1.

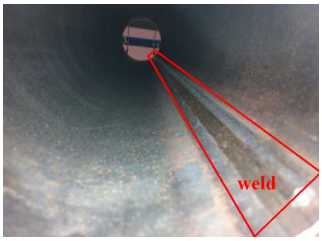

Figure C1: The welding line in the cylinder

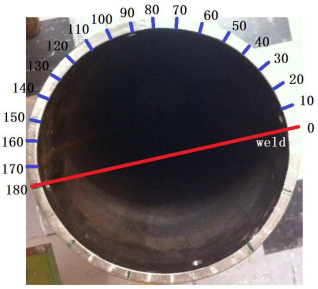

Figure C2: Details of the cross section measurement

Table C1: Inner and outer diameters of the cross sections

Top End			Bottom End		
degree	Diameter(m)		degree	Diameter(m)	
	inner	outer		inner	outer
0	0.1544	0.1680	0	0.1540	0.1685
10	0.1545	0.1681	10	0.1545	0.1680
20	0.1543	0.1681	20	0.1545	0.1681
30	0.1545	0.1680	30	0.1544	0.1685
40	0.1548	0.1684	40	0.1545	0.1685
50	0.1547	0.1685	50	0.1542	0.1682
60	0.1543	0.1681	60	0.1538	0.1675
70	0.1539	0.1677	70	0.1535	0.1673
80	0.1538	0.1677	80	0.1539	0.1675
90	0.1539	0.1680	90	0.1540	0.1676
100	0.1540	0.1680	100	0.1543	0.1680
110	0.1543	0.1686	110	0.1549	0.1687
120	0.1545	0.1688	120	0.1545	0.1685
130	0.1545	0.1685	130	0.1543	0.1682
140	0.1542	0.1681	140	0.1540	0.1680
150	0.1540	0.1680	150	0.1537	0.1678
160	0.1539	0.1681	160	0.1540	0.1680
170	0.1543	0.1684	170	0.1540	0.1680

REFERENCES

[1] Laura P.A.A, Filipich C.P, Rossi R.E, Reyes J.A. 1988, "*Vibrations of rings of variable cross section*",Applied Acoustics, Vol.125, pp. 225–234.

[2] Hwang R.S, Fox C.H.J, McWilliam S. 1999, "*The in-plane vibration of thin rings within-plane profile variations —part I: general background and theoretical formulation*", Journal of Sound and Vibration, Vol.220, no.3, pp. 497–516.
[3] Khurasia H. B, Rewtant S. 1978, "*Vibration analysis of circular plates with hole*", Journal of Applied Mechanics, Vol.45, pp. 215–217.
[4] Hasheminejad Seyyed M, Mirzaei Yaser.2009, "*Free vibration analysis of an eccentric hollow cylinder using exact 3D elasticity theory*", Journal of Sound and Vibration, Vol.326, no.3-5, pp. 687–702.
[5] Lombard M.2008, *SolidWorks 2007 Bible*, Hoboken: John Wiley & Sons, Inc.
[6] Hatch M.R.2001,*Vibration simulation using MATLAB and ANSYS*, Boca Raton: Chapman & Hall/CRC.
[7] Liu Wei, Pan Jie, Matthews David. 2010, *"Measurement of sound-radiation from a torpedo-shaped structure subjected to an axial excitation*", Proceedings of the 20th International Congress on Acoustics, ICA 2010, 23-27 August 2010, Sydney, Australia.
[8] Yamada G, Irie T, Tagawa Y.1984, "*Free vibration of non-circular cylindrical shells with variable circumferential profile"*, Journal of Sound and Vibration,Vol.95, no.1, pp.117-126.